ISSN 2411-3336; e-ISSN 2541-9404

JOURNAL OF MINING INSTITUTE

Zapiski Gornogo instituta

Journal homepage: pmi.spmi.ru



Research article

Trace elements in the silicate minerals of the Borodino Meteorite (H5)

Kristina G. SUKHANOVA
Institute of Precambrian Geology and Geochronology RAS, Saint Petersburg, Russia

How to cite this article: Sukhanova K.G. Trace elements in the silicate minerals of the Borodino Meteorite (H5). Journal of Mining Institute. 2024. Vol. 265, p. 16-33. EDN WHSYGT

Abstract. Major (EPMA) and trace (SIMS) element geochemistry in olivine, low-Ca pyroxene and mesostasis from porphyritic and barred chondrules, as well as the pyroxene-olivine aggregate and matrix of equilibrated ordinary Borodino chondrite (H5) is discussed. No differences in major element concentrations in the silicate minerals of the chondrules and matrix of the meteorite were found. The minerals of porphyritic olivine-pyroxene and barred chondrules display elevated trace element concentrations, indicating the rapid cooling of chondrule melt in a nebula, and are consistent with experimental data. The trace element composition of low-Ca pyroxene is dependent on the position of a pyroxene grain inside a chondrule (centre, rim, matrix) and the composition of mesostasis is controlled by the type of the object (porphyritic and barred chondrules, pyroxene-olivine aggregate). The depletion in trace elements of low-Ca pyroxene from the rims of chondrules in comparison with those from the centre and matrix of the meteorite was revealed. The chondrule rim is affected by interaction with surrounding gas in a nebula, possibly resulting in the exchange of moderately volatile trace elements in low-Ca pyroxene and depletion in these elements relative to pyroxene from the centre of the chondrule or matrix of the meteorite. The mesostasis of barred and porphyritic olivine-pyroxene chondrules contains more trace elements than that of porphyritic olivine chondrule and pyroxene-olivine aggregate, suggesting the rapid cooling of these objects or their high liability to thermal metamorphism, which results in the recrystallization of chondrule glass into plagioclase. However, no traces of the elevated effect of thermal metamorphism on the above objects have been revealed. The results obtained indicate no traces of the equilibration of the trace element composition of silicate minerals in equilibrated chondrites.

Keywords: ordinary chondrites; trace elements; olivine; pyroxene; mesostasis; ion probe

Acknowledgment. The study was carried out within the framework of the research topic of the IPGG RAS FMUW-2022-0005.

Received: 04.04.2023 ***Accepted: 20.06.2023*** ***Online: 09.10.2023*** ***Published: 29.02.2024***

Introduction. The Borodino Meteorite is one of few meteorites with a unique history. The history of its finding and living on the Earth is unusual. The meteorite fell at night on the eve of the Borodino Battle, on September 5, 1812, near the village of Gorky [1]. The stone was picked up by a Russian soldier who was on duty. The soldier gave the stone to Major Christian Ivanovich Dieterichs. Major Dieterichs was wounded on the battle field. After resigning, he lived in his estate in Kurlandia (modern Latvia) [2]. The Major's family kept the meteorite for 80 years, in 1890, Gerke, manager of the son of Major Dieterichs, donated a large piece of meteorite (320 g) to the Mining Institute museum. However, a small piece was owned by Y.I.Simashko, an entomologist, a writer and a publisher. Simashko described the meteorite's history in a letter to the British Museum of Natural History [3].

The Borodino Meteorite is an equilibrated ordinary chondrite, the most common type of meteorites known on Earth [4]. Chondrites consist of silicate spherules (chondrules), less than one millimeter in size, which occur in a weightless nebula of melt drops consisting of olivine, low-Ca pyroxene and mesostasis. Structurally, chondrules are subdivided into a porphyritic type composed of olivine and/or pyroxene phenocrysts and a nonporphyritic type (barred, radiated-structured, cryptocrystalline, etc.).

This is an open access article under the CC BY 4.0 license

Journal of Mining Institute. 2024. Vol. 265. P. 16-33
© Kristina G. Sukhanova, 2024

A variety of chondrule structures suggests a variety of the cooling conditions of the melt. Experiments have shown that porphyritic chondrules are formed from slowly cooling melt (1-500 °C/h), which was heated below liquidus temperature (1400-1700 °C) and preserved an abundance of relict grains. The crystallization of barred chondrules requires the heating of the melt at temperatures slightly above liquidus temperature followed by rapid cooling (500-3000 °C/h). Radial chondrules suggest that melt was subjected to high temperatures and then cooled instantaneously (1000-3000 °C/h) [5].

The sample taken from the Borodino Meteorite mainly contains olivine and olivine-pyroxene porphyritic chondrules. Barred and cryptocrystalline chondrules are scarce.

The porphyritic chondrules of unaltered ordinary chondrites (UOC) occasionally display isolated MgO-enriched refractory olivine grains, differing in the isotopic composition of oxygen from chondrule olivine [6, 7], and MgO-richer olivine grain cores overgrown with MgO-poorer forsterite rims [8]. The presence of relict olivine grains in porphyritic chondrules suggests that they were produced by the melting of precursor minerals, such as refractory inclusions (e,g, calcium-aluminium and amoeba-like olivine inclusions) [9], the fine-grained material of chondrite matrix and fragments of previous generations of chondrules, fragments of planetesimals [10], H_2O ice [11], "relict" olivine and dust clusters [12].

Chondrules from ordinary chondrites occur among single grains of silicate minerals, troilite, kamacite-taenite, chromite and other minerals, making up meteorite matrix. The Borodino Meteorite matrix consists of coarse well-defined grains of minerals commonly occurring in the matrix of chondrites. The chondrule-matrix boundaries are well defined. No veinlets or melting pockets have been revealed.

Most of ordinary chondrites show traces of thermal metamorphism, which took place on fairly big (over 50 km in diameter) parent bodies. Thermal metamorphism resulted in the homogenization (equilibration) of Fe-Mg in olivine and low-Ca pyroxene, the recrystallization of mesostasis into plagioclase, the formation of high-Ca pyroxene, apatite and chromite and the obliteration of chondrule-matrix boundaries [13]. The petrologic type (p.t.) of ordinary chondrite is identified from the petrographic characters and compositional variability of silicate minerals. UOC's are of three petrologic types. Their Fe and Mg concentrations in olivine and low-Ca pyroxene are most variable. The variability of Fe and Mg in the fourth to a sixth p.t. fades out gradually (ordinary equilibrated chondrites – EOC), giving way to other signs of thermal metamorphism. The Borodino Meteorite (H5) is of a fifth p.t. and the high-Fe group (H) of EOC.

In spite of an abundance of EOC, which make up over 90 % of all meteorites found, they are poorly understood. Thermal metamorphism disturbed the original distribution of chemical elements and their isotopes in EOC minerals, they were not used for the study of chondrule formation and accretion. However, trace elements in silicate minerals are practically immobile on parental chondrite bodies affected by thermal metamorphism [14, 15]. Therefore, they are used for the study of early stages in the formation of the Solar System [16-18]. The study of the composition of refractory trace elements in olivine, pyroxene and the glass of UOC chondrules has revealed various types of porphyritic chondrule crystallization [19] making it possible to calculate their relative cooling rates [20-22]. The composition of moderately volatile trace elements usually indicates the interaction of a chondrule with surrounding gas in a protoplanetary disk [23].

Trace and rare-earth elements are widely used for the study of geochemical settings, in which genetically different minerals, such as zircon [24, 25], beryl [26, 27], olivine [28], etc., were formed.

Pioneer studies on the compositions of the silicate minerals of EOC showed heterogeneous trace element concentrations [29, 30] and oxygen isotope ratios [31] in the olivine and pyroxene of EOC. The trace element composition of silicate minerals from Borodino Meteorite chondrules will be

This is an open access article under the CC BY 4.0 license

analyzed to assess the effect of thermal metamorphism on trace element concentrations and to reveal differences in the settings in which structurally different chondrules were formed.

Analytical methods. A sample of the Borodino chondrite (H5) was provided by the Mining Museum of Saint Petersburg Mining University. The chemical composition of minerals at the level of major elements was determined using the EPMA method at IGGD RAS on a Jeol JXA-8230 microprobe analyzer with five wave spectrometers. The meteorite substance was placed in a standard epoxy resin mould sprayed with carbon after polishing. Point measurements of mineral compositions were carried out at an accelerating voltage of 20 kV and a current of 20 nA for olivine and pyroxene and at 10 nA for mesostasis [32]. The focused beam was 3 μm in diameter. Natural minerals, pure oxides and metals were used as standards. ZAF algorithm was used for correcting the matrix effect. Kα1 lines were measured for all elements.

Trace and rare-earth element (REE) concentrations in minerals were identified using the secondary ion mass spectrometry (SIMS) method on a Cameca IMS-4f ion microprobe at the Yaroslavl Branch of K.A.Valiev Physico-Technological Institute, RAS, using the technique described in [33]. The preparation was sprayed with gold prior to measurements. Survey on a Cameca IMS-4f ion microprobe was done under the following conditions: a primary ion beam was $16O_2^-$, beam diameter was ~20 μm; ion current was 5-7 nA; and the accelerating voltage of the primary beam was 15 keV. The measurement error was no more than 10 % for impurities with concentrations over 1 ppm and 20 % for concentrations of less than 1 ppm. The trace element composition of rock-forming minerals was analyzed as close as possible to the analytical points of major elements using the EPMA method. REE distribution spectra in minerals were CI chondrite-normalized [34].

Results. Two porphyritic and one barred chondrules, as well as olivine-pyroxene aggregate, from the Borodino Meteorite were studied. The porphyritic chondrules display olivine composition for 14PO-4 and olivine-pyroxene composition for 14POP-1. Barred chondrule 14BOP-2 consists of thin parallel olivine and low-Ca pyroxene bars. The porphyritic chondrules measure about 0.5 mm and a barred chondrule is over 1 mm in size. No well-defined metallic and silicate rims of the chondrules were revealed, but coarse kamacite-taenite and troilite grains are occasionally encountered at the chondrule-matrix boundary.

Pyroxene-olivine aggregate 14APO-3 consists of coarse low-Ca pyroxene grains overgrowing fine olivine grains in the centre of the aggregate. Coarse kamacite-taenite grains and fine troilite grains occur along the aggregate boundaries. The contours of the aggregate resemble the rounded shape of the chondrules, suggesting the recrystallization and coarsening of chondrule minerals as a result of thermal metamorphism on the parent body. However, the complete absence of mesostasis in the aggregate is not typical of chondrules.

Chondrule 14POP-1 has a rounded shape, a porphyritic structure and a small size (0.5 mm). It consists of coarse olivine phenocrysts occurring in the centre of the chondrule and evenly distributed low-Ca pyroxene grains. Olivine also occurs as fine grains near the chondrule boundary. Mesostasis fills interstices between olivine and pyroxene, typically occurring in the centre of the chondrule. The matrix surrounding the chondrule consists of equigranular material composed of olivine and low-Ca pyroxene. Mesostasis is scarce.

Olivine in porphyritic chondrule 14POP-1 was identified as forsterite (Fo 81). It occurs as a coarse (200 μm lengthwise) idiomorphic grain in the centre and fine (50-100 μm) hypidiomorphic grains near chondrule rims (Fig.1). Major element concentrations are practically invariable. There is no difference in olivine composition between the chondrule and the matrix (Table 1). Trace element concentrations in olivine vary markedly: refractory Zr and Ti, as well as moderately volatile Ba, V, Ni, Cr and REE, vary by several orders of magnitude. The highest trace element concentrations are exhibited by olivine at the chondrule rim, where Zr, Hf, REE and Sr concentrations are more than twice as high as those of olivine in the centre of the chondrule and matrix of the meteorite.

This is an open access article under the CC BY 4.0 license

Journal of Mining Institute. 2024. Vol. 265. P. 16-33
© Kristina G. Sukhanova, 2024

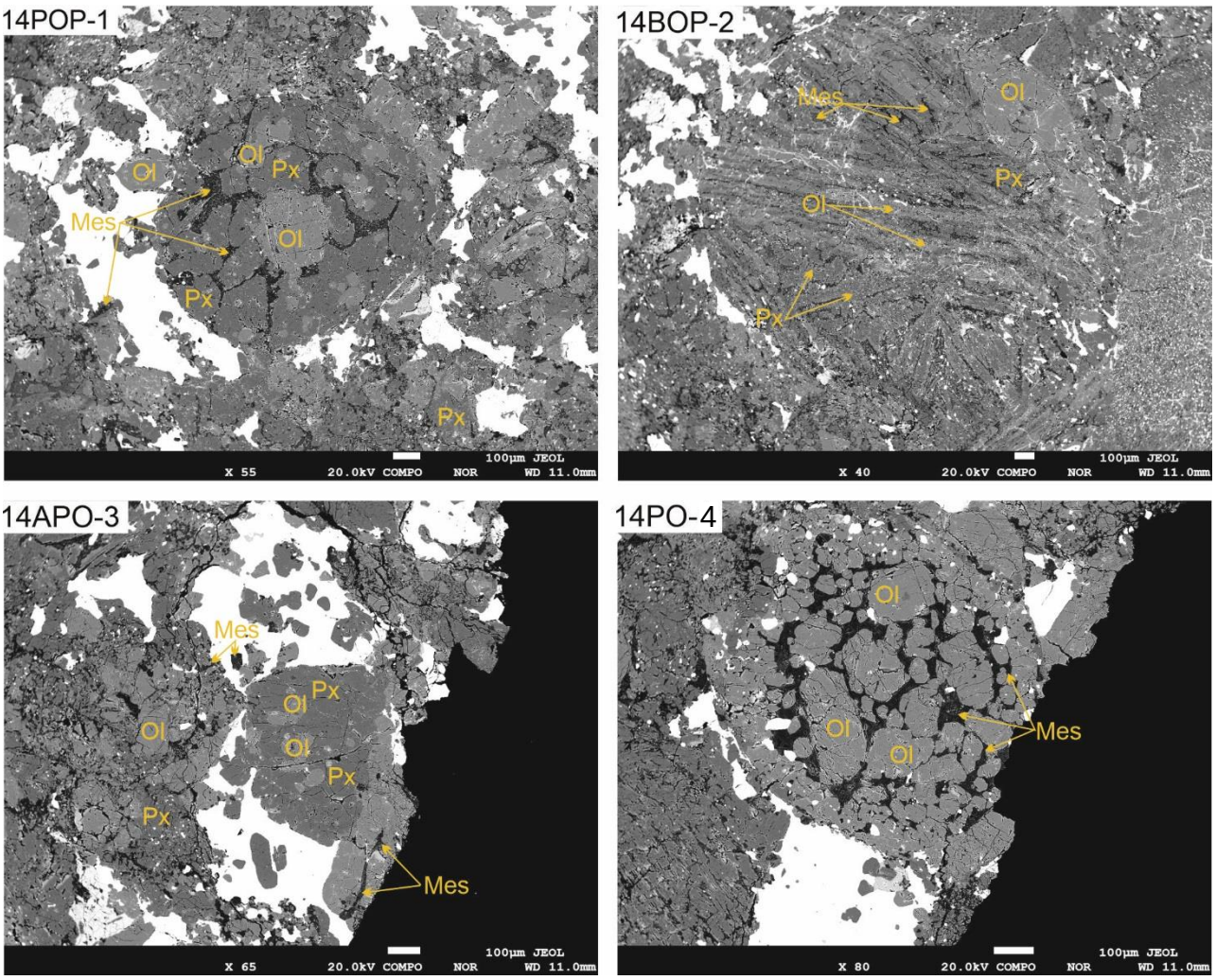


Fig.1. BSE images of chondrules of the Borodino Meteorite:
Ol – olivine, Px – low-Ca pyroxene, Mes – mesostasis

Table 1

Major (wt.%) and trace (ppm) element composition of silicate minerals from 14POP-1 chondrule of the Borodino Meteorite

Component	Ol			Px			Mes		
	Centre	Rim	Matrix	Centre	Rim	Matrix	Rim	Rim	Matrix
SiO_2	39.38	39.60	39.23	57.87	57.70	56.76	63.13	64.22	64.26
Al_2O_3	0.00	0.02	0.01	0.12	0.10	0.24	19.64	19.38	21.46
MgO	43.27	43.60	42.78	30.44	30.84	30.34	1.31	0.36	0.30
TiO_2	0.00	0.00	0.02	0.11	0.11	0.20	0.38	1.89	0.02
CaO	0.02	0.01	0.03	0.60	0.56	0.72	4.30	1.96	2.90
FeO	17.55	17.40	17.63	10.96	11.15	10.94	1.80	1.45	0.58
MnO	0.49	0.46	0.48	0.53	0.51	0.51	–	–	–
Cr_2O_3	0.02	0.02	0.02	0.11	0.08	0.31	–	–	–
NiO	0.00	0.01	0.00	0.00	0.01	0.02	–	–	–
Na_2O	–	–	–	–	–	–	9.75	10.07	9.78
K_2O	–	–	–	–	–	–	0.56	1.55	0.65
Total	100.74	101.11	100.19	100.73	101.04	100.05	100.86	100.87	99.95
Zr	1.06	5.28	2.05	21.4	2.05	8.01	61.7	61.8	112
Hf	b.d.l.	0.25	0.11	0.45	0.09	0.18	1.45	1.39	3.03
Ca	4299	3987	6230	5210	5524	5821	–	–	–
Y	0.03	0.08	0.08	0.36	0.18	0.31	1.61	2.09	1.30

This is an open access article under the CC BY 4.0 license

End of Table 1

Component	Ol			Px			Mes		
	Centre	Rim	Matrix	Centre	Rim	Matrix	Rim	Rim	Matrix
Al	165	155	110	612	696	1181	–	–	–
Ti	80.8	104	326	894	732	1077	2009	1776	1454
Nb	0.40	0.09	0.19	0.33	0.17	0.41	1.63	1.05	2.02
La	0.01	0.26	0.12	1.15	0.04	0.27	2.81	2.99	3.12
Ce	0.02	0.60	0.20	2.38	0.11	0.50	4.60	3.79	5.76
Pr	b.d.l.	0.04	0.03	0.22	0.01	0.06	0.59	0.52	0.62
Nd	b.d.l.	0.24	0.13	0.89	0.06	0.27	2.12	2.26	2.35
Sm	b.d.l.	0.06	0.04	0.14	0.07	0.04	0.32	0.14	0.25
Eu	0.01	0.03	0.01	0.04	0.01	0.01	0.27	0.15	0.76
Gd	0.03	0.27	0.02	0.13	0.04	0.07	0.36	0.16	0.45
Tb	–	–	–	–	–	–	–	–	–
Dy	b.d.l.	b.d.l.	b.d.l.	0.07	b.d.l.	0.06	0.33	0.28	0.18
Ho	–	–	–	–	–	–	–	–	–
Er	b.d.l.	b.d.l.	b.d.l.	0.04	0.06	0.07	0.26	0.17	0.09
Yb	0.03	0.05	0.02	0.14	0.06	0.09	0.17	0.26	0.16
Lu	0.01	0.01	0.01	0.02	0.02	0.03	0.03	0.04	0.03
Sr	0.10	1.20	1.47	0.40	0.49	0.88	28.4	23.3	104
Ba	0.12	6.79	1.53	4.10	0.37	4.00	14.9	12.9	34.7
V	45.7	14.3	34.0	64.0	47.6	133	102	126	64.7
Ni	17.9	103	53.2	50.6	56.7	160	–	–	–
Cr	1939	316	1546	2733	1583	5921	3133	2881	1793
Rb	2.36	1.66	3.22	0.57	1.47	1.76	5.34	8.31	14.1
REE	0.12	1.56	0.57	5.21	0.48	1.49	11.8	10.8	13.8
LREE	0.05	1.23	0.53	4.82	0.30	1.16	10.7	9.86	12.9
HREE	0.07	0.33	0.04	0.39	0.18	0.33	1.14	0.91	0.90

Note. Dash – no element detected; b.d.l. – element content is below the detection limit.

Trace element distribution spectra for olivine are mildly differentiated (Fig.2, *a*). Trace element concentrations in olivine at the rim of chondrule 14POP-1 in the Borodino Meteorite practically reach chondrite values, which is not typical of olivine from ordinary chondrites. Olivine from chondrule 14POP-1 displays higher trace element concentrations than those in olivine from UOC, except for Al. Al concentration in olivine from the chondrule and the matrix is less by one order of magnitude than Al concentration in olivine from UOC.

Olivine from chondrule 14POP-1 is also richer in REE than olivine from UOC, although it typically displays the prevalence of heavy rare-earth elements (HREE) over light (LREE). Olivine from the matrix shows the prevalence of LREE.

Low-Ca pyroxene from chondrule 14POP-1 occurs as enstatite (En 81, Wo 1). It is evenly distributed over the chondrule area, occurring as fine (about 100 μm lengthwise) idiomorphic and hypidiomorphic grains. Major element concentrations vary slightly. Pyroxene from the chondrule does not differ in major element concentrations, but pyroxene from the matrix is twice as rich in Al and Ti as pyroxene from the chondrule.

Trace element concentrations in low-Ca pyroxene are relatively stable. Elevated Zr and Ce concentrations in pyroxene from the centre of the chondrule (21.4 and 2.38 ppm, respectively) and low REE concentrations (0.48 ppm) in the pyroxene of the chondrule rim were revealed.

Trace element distribution spectra for low-Ca pyroxene from chondrule 14POP-1 are poorly differentiated (Fig.2, *c*). They differ mainly in REE concentrations. For instance, pyroxene from the centre of the chondrule and the matrix typically displays the prevalence of LREE over HREE, but pyroxene from the chondrule rim exhibits elevated HREE concentrations relative to LREE. Pyroxene from the meteorite matrix displays a positive europium anomaly.

Pyroxene in chondrule 14POP-1 is richer in refractory trace elements and REE than low-Ca pyroxene from UOC, except for Al. Moderately volatile element concentrations in pyroxene from chondrules 14POP-1 and UOC are practically the same.

This is an open access article under the CC BY 4.0 license

Journal of Mining Institute. 2024. Vol. 265. P. 16-33
© Kristina G. Sukhanova, 2024

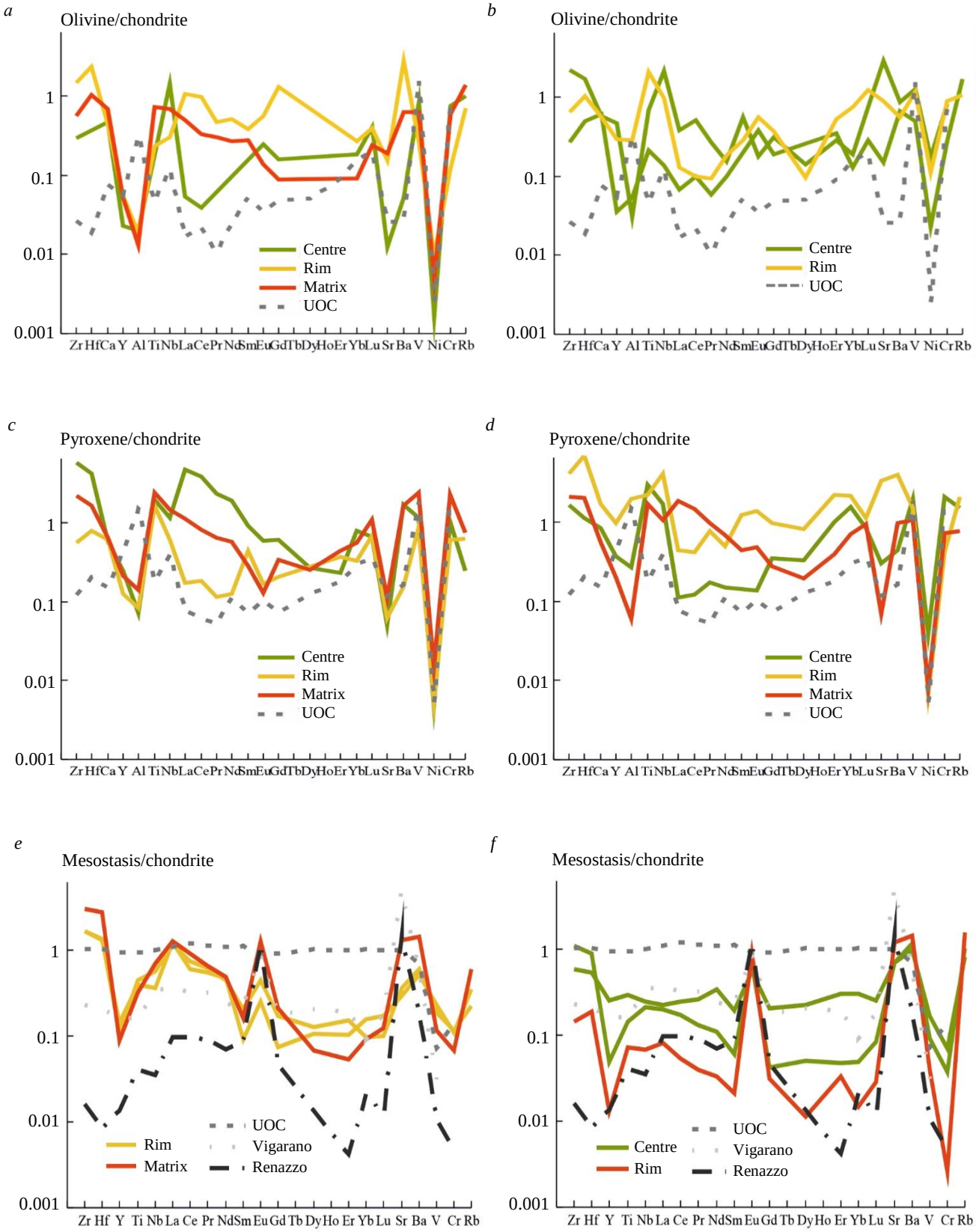


Fig.2. Spider diagrams for trace elements normalized to CI chondrite. Chondrule 14POP-1: olivine (*a*); low-Ca pyroxene (*c*) and mesostasis (*e*). Chondrule 14BOP-2: olivine (*b*); low-Ca pyroxene (*d*) and mesostasis (*f*). Data on the composition of UOC minerals are given according to [20, 21]

This is an open access article under the CC BY 4.0 license

Mesostasis from chondrule 14POP-1 consists of highly recrystallized glass of albite (An 8 Or 8) and oligoclase (An 19 Or 3) composition. It fills large interstices between olivine and pyroxene, and is more abundant near the chondrule rim. The mesostasis contains acicular aggregates of high-Ca pyroxene and micron-sized chromite and troilite grains. Its slightly variable major element composition is due to the heterogeneity of the mesostasis. MgO 0.30-1.31 (wt.%) and TiO_2 concentrations (0.02-1.89 wt.%) are most variable.

Trace elements in the mesostasis of chondrule 14POP-1 vary slighly. Mesostasis from the meteorite matrix is slightly enriched in Zr and moderately volatile elements (Sr, Ba, V and Rb). Trace element concentrations in mesostasis from the chondrule remains unchanged in spite of its heterogeneity.

Trace element distribution spectra for mesostasis from chondrule 14POP-1 fully coincide with those for plagioclase from Vigarano coaly chondrule, but contain more Zr, Hf and LREE (Fig.2, *e*).

Barred chondrule 14BOP-2 consists of thin olivine and low-Ca pyroxene bars. Small interstices between them are filled with mesostasis. The chondrule is over 1 mm in size, has no metallic or silicate rims, is rounded in shape and the chondrule-matrix boundary is poorly-defined (see Fig.1).

Olivine in barred chondrule 14BOP-2 is present as forsterite (Fo 81). It occurs as thin highly elongated (from one chondrule rim to the other) inequidirectional skeletal crystals and is evenly distributed throughout the chondrule. Major element concentrations in olivine are practically invariable, except for FeO and MgO, which is typical of a meteorite of a fifth petrologic type (Table 2).

Trace elements in olivine from the chondrule also vary slightly. Olivine grains depleted in refractory elements (Y, Al, Ti, Nb) occur in the centre of the chondrule. Olivine from the chondrule rim is slightly different in trace element concentrations from that in the centre of the chondrule.

Trace element distribution spectra for olivine from the chondrule are poorly differentiated (Fig.2, *b*). No significant differences between olivine from the centre and rim of the chondrule were revealed. Olivine from chondrule 14BOP-2 contains higher trace and rare-earth element concentrations than olivine from UOC. Al concentration in olivine from the chondrule rim is similar to that in olivine from UOC, a feature not typical of olivine from other chondrules.

Low-Ca pyroxene from the chondrule is present as enstatite (En 81, Wo 1). Like olivine, it forms skeletal crystals elongated from one chondrule rim to the other. It mainly occurs in the centre of chondrules. Pyroxene occasionally has thin ore mineral (kamacite-taenite, chromite and troilite) streaks. Major element concentrations in low-Ca pyroxene from the chondrule and matrix of the meteorite are stable.

Trace elements in low-Ca pyroxene from the barred chondrule varies slightly, depending on the position of pyroxene in the chondrule. Pyroxene from the centre of the chondrule is depleted in LREE and contains low refractory trace element (Zr, Al, Ca) concentrations. Pyroxene from the chondrule rim is richer in refractory and rare-earth elements than pyroxene from the centre and matrix of the meteorite. Low-Ca pyroxene from the matrix has low Al and HREE concentrations.

Trace element distribution spectra for low-Ca pyroxene from chondrule 14BOP-2 are poorly differentiated, and trace element concentrations are close to chondrite values (Fig.2, *d*). HREE's typically prevail over LREE's in pyroxene from the chondrule, but pyroxene from the matrix displays an inverse trend.

Low-Ca pyroxene from the barred chondrule is richer in refractory and rare-earth elements than low-Ca pyroxene from UOC, although pyroxene from the chondrule is poor in Al than pyroxene from UOC.

Mesostasis fills micron-sized interstices between olivine and pyroxene bars. The aggregates are no more than 50 μm in size. The mesostasis on BSE-images generally looks homogeneous, although it often occurs with fine ore mineral grains. In chondrule 14BOP-2, mesostasis is present as poorly recrystallized glass of oligoclase composition (An 11 Or 5). In the matrix, its composition may vary to anorthoclase (An 7 Or 13). The minor element composition of the mesostasis is invariable, except for FeO and MgO.

This is an open access article under the CC BY 4.0 license

Journal of Mining Institute. 2024. Vol. 265. P. 16-33
© Kristina G. Sukhanova, 2024

Table 2

Major (wt.%) and trace (ppm) element composition of silicate minerals from 14BOP-2 chondrule of the Borodino Meteorite

Component	Ol			Px			Mes		
	Centre	Centre	Rim	Centre	Rim	Matrix	Centre	Centre	Matrix
SiO_2	39.82	39.16	39.59	57.65	57.23	57.45	64.79	63.68	63.37
Al_2O_3	0.01	0.01	0.00	0.16	0.16	0.12	20.97	19.84	20.22
MgO	42.71	42.18	43.57	30.42	30.77	30.78	0.07	0.32	1.08
TiO_2	0.00	0.00	0.01	0.14	0.16	0.10	0.00	0.06	0.04
CaO	0.02	0.05	0.02	0.68	0.70	0.72	2.46	2.42	2.50
FeO	17.93	18.37	17.21	11.04	11.26	11.06	0.89	2.26	1.32
MnO	0.47	0.47	0.50	0.51	0.48	0.47	–	–	–
Cr_2O_3	0.00	0.06	0.00	0.21	0.15	0.14	–	–	–
NiO	0.01	0.18	0.00	0.01	0.02	0.04	–	–	–
Na_2O	–	–	–	–	–	–	10.36	9.90	8.94
K_2O	–	–	–	–	–	–	0.81	1.04	1.10
Total	100.97	100.47	100.90	100.83	100.93	100.87	100.33	99.51	98.57
Zr	0.96	8.10	2.36	5.93	15.0	7.49	21.6	40.2	5.18
Hf	0.05	0.18	0.11	0.12	0.74	0.22	0.58	0.97	0.20
Ca	5626	5320	5035	7713	15349	5080	–	–	–
Y	0.05	0.68	0.43	0.54	1.44	0.29	3.69	0.72	0.19
Al	452	257	2417	2239	16514	509	–	–	–
Ti	94.7	308	939	1317	990	752	1326	642	328
Nb	0.04	0.60	0.27	0.49	1.18	0.30	0.71	0.60	0.20
La	0.02	0.09	0.03	0.03	0.11	0.45	0.55	0.48	0.20
Ce	0.06	0.32	0.06	0.08	0.26	0.90	1.56	1.09	0.33
Pr	0.01	0.03	0.01	0.02	0.07	0.09	0.25	0.12	0.04
Nd	0.05	0.07	0.09	0.07	0.24	0.33	1.62	0.52	0.16
Sm	b.d.l.	0.09	0.04	b.d.l.	0.19	0.07	0.30	0.09	0.03
Eu	0.02	0.01	0.03	0.01	0.08	0.03	0.32	0.40	0.52
Gd	0.04	0.06	0.08	0.07	0.20	0.06	0.43	0.09	0.06
Tb	–	–	–	–	–	–	–	–	–
Dy	b.d.l.	0.04	0.02	0.08	0.21	0.05	0.57	0.13	0.03
Ho	–	–	–	–	–	–	–	–	–
Er	0.06	0.05	0.09	0.17	0.37	0.07	0.51	0.08	0.06
Yb	0.02	0.03	0.13	0.26	0.36	0.12	0.52	0.08	0.02
Lu	0.01	0.02	0.03	0.02	0.03	0.02	0.06	0.02	0.01
Sr	1.18	22.2	6.90	2.35	26.4	0.55	55.5	56.0	93.7
Ba	1.59	2.09	1.35	1.07	9.62	2.39	24.1	28.2	35.4
V	27.5	70.2	63.9	109	81.9	57.5	91.7	50.5	21.8
Ni	248	1910	1200	424	73.3	90.2	–	–	–
Cr	727	2176	2326	5498	1097	1917	1851	991	68.5
Rb	3.98	b.d.l.	2.48	3.51	4.82	1.77	18.8	24.5	36.6
REE	0.28	0.80	0.61	0.81	2.11	2.18	6.70	3.12	1.46
LREE	0.15	0.60	0.27	0.20	0.95	1.86	4.60	2.71	1.28
HREE	0.13	0.20	0.35	0.61	1.16	0.32	2.10	0.40	0.18

Trace element concentrations vary considerably. For instance, mesostasis from the centre of the chondrule is richer in refractory trace elements than that from the meteorite matrix. There are also some differences between mesostasis grains in the centre of the chondrule. FeO-depleted mesostasis contains higher refractory and rare-earth concentrations than other central mesostasis grains.

The trace element distribution spectra are highly differentiated (Fig.2, *f*). Mesostasis from the matrix is poor in trace elements. The spectra clearly show the prevalence of LREE over HREE and a well-defined europium anomaly. Mesostasis from the matrix coincides largely with a trace element distribution spectrum for plagioclase from Renazzo coaly chondrite. However, it contains high refractory element (Zr, Hf and Ti) and low REE concentrations. Mesostasis from chondrule 14BOP-2 shows a trace element distribution spectrum similar to that for plagioclase from the Vigarano Meteorite, although it seems to decline towards the Renazzo spectrum, occupying an intermediate position.

This is an open access article under the CC BY 4.0 license

© Kristina G. Sukhanova, 2024

Pyroxene-olivine aggregate 14APO-3 was formed as the isometric intergrowth of fine (250-300 μm) low-Ca crystals with hypidiomorphic olivine grains (50-100 μm) (see Fig.1) in its centre. Mesostasis from the aggregate is poorly-defined. It mainly occurs at the matrix-aggregate boundary. The aggregate could be interpreted as a highly metamorphosed chondrule with completely obliterated boundaries. However, it is hardly a chondrule, because its rims are not rounded and its internal structure is specific.

Olivine from the aggregate is present as forsterite (Fo 81). It occurs as several grains located mainly in the centre of the aggregate. The major element composition of olivine is stable.

Trace element concentrations in olivine from the aggregate are slightly variable (Table 3). Olivine from aggregate 14APO-3 tends to be slightly richer in trace elements than olivine from the matrix. However, no significant differences in trace element concentrations were revealed.

Table 3

Major (wt.%) and trace (ppm) element composition of silicate minerals from aggregate 14APO-3 chondrule of the Borodino Meteorite

Component	Ol			Px			Mes		
	Centre	Centre	Matrix	Rim	Rim	Matrix	Centre	Rim	Matrix
SiO_2	39.37	39.33	39.70	56.64	57.40	57.71	65.32	64.27	65.61
Al_2O_3	0.02	0.00	0.00	0.21	0.14	0.12	20.98	21.02	19.95
MgO	42.77	43.10	42.91	30.95	30.24	30.43	0.18	0.10	0.39
TiO_2	0.01	0.00	0.02	0.22	0.14	0.14	0.07	0.01	0.01
CaO	0.04	0.01	0.03	0.74	0.74	0.76	2.43	2.41	1.48
FeO	17.90	17.78	17.86	11.26	11.12	11.02	0.65	2.26	0.77
MnO	0.48	0.48	0.46	0.50	0.47	0.49	–	–	–
Cr_2O_3	0.03	0.02	0.01	0.22	0.17	0.13	–	–	–
NiO	0.01	0.02	0.00	0.02	0.00	0.00	–	–	–
Na_2O	–	–	–	–	–	–	10.15	10.15	9.25
K_2O	–	–	–	–	–	–	0.97	0.89	2.41
Total	100.61	100.72	100.98	100.75	100.42	100.80	100.74	101.11	99.86
Zr	0.33	1.25	0.48	0.88	0.41	2.13	2.30	7.43	9.20
Hf		0.09	0.06	0.05	0.14	0.10	b.d.l.	0.29	0.25
Ca	4538	4529	4189	5506	4657	5063	–	–	–
Y	0.02	0.10	0.06	0.29	0.23	0.31	0.15	0.30	0.59
Al	76.5	221	38.0	649	422	784	–	–	–
Ti	103	390	45.2	1028	701	1156	303	319	469
Nb	0.08	0.08	0.06	0.03	0.05	0.16	0.23	0.42	0.47
La	0.02	0.01	0.01	0.04	0.01	0.03	0.11	0.25	0.11
Ce	0.02	0.03	0.02	0.06	0.02	0.05	0.15	0.35	0.31
Pr	0.01	0.01	0.01	0.01	0.00	0.01	0.01	0.04	0.03
Nd	b.d.l.	0.05	b.d.l.	0.10	b.d.l.	0.06	0.06	0.21	0.09
Sm	0.05	b.d.l.	0.04	0.04	b.d.l.	0.05	b.d.l.	0.06	0.04
Eu	0.01	b.d.l.	b.d.l.	0.01	b.d.l.	0.02	0.49	0.59	0.41
Gd	0.02	0.02	b.d.l.	0.02	0.02	0.02	0.02	0.03	0.06
Tb	–	–	–	–	–	–	–	–	–
Dy	–	0.03	0.03	0.05	0.03	0.03	0.02	0.06	0.07
Ho	–	–	–	–	–	–	–	–	–
Er	b.d.l.	0.01	0.04	0.11	0.03	0.07	0.08	0.03	0.04
Yb	0.06	0.04	0.03	0.07	0.07	0.11	0.03	0.03	0.06
Lu	b.d.l.	b.d.l.	0.01	0.02	0.01	0.01	0.01	0.01	0.01
Sr	0.09	0.28	0.21	0.14	0.12	0.34	82.7	100	76.4
Ba	0.21	0.58	0.25	0.28	0.20	0.55	33.8	42.5	40.0
V	17.3	31.1	24.1	50.5	39.9	56.0	21.0	26.2	41.3
Ni	27.4	121	64.8	40.4	49.4	89.2	–	–	–
Cr	459	648	430	1080	962	1181	146	113	330
Rb	1.55	1.70	2.91	0.73	0.97	1.21	25.6	28.6	248
REE	0.20	0.21	0.20	0.53	0.20	0.47	0.98	1.67	1.23
LREE	0.11	0.10	0.09	0.26	0.03	0.22	0.82	1.50	0.99
HREE	0.09	0.10	0.11	0.27	0.17	0.25	0.16	0.17	0.24

This is an open access article under the CC BY 4.0 license

Journal of Mining Institute. 2024. Vol. 265. P. 16-33
© Kristina G. Sukhanova, 2024

The trace element distribution spectrum for the aggregate is slightly fractionated. Trace element concentrations in olivine are below chondrite values (Fig.3, *a*). Olivine from aggregate 14APO-3 is richer in refractory and rare-earth elements than olivine from UOC, except for Al.

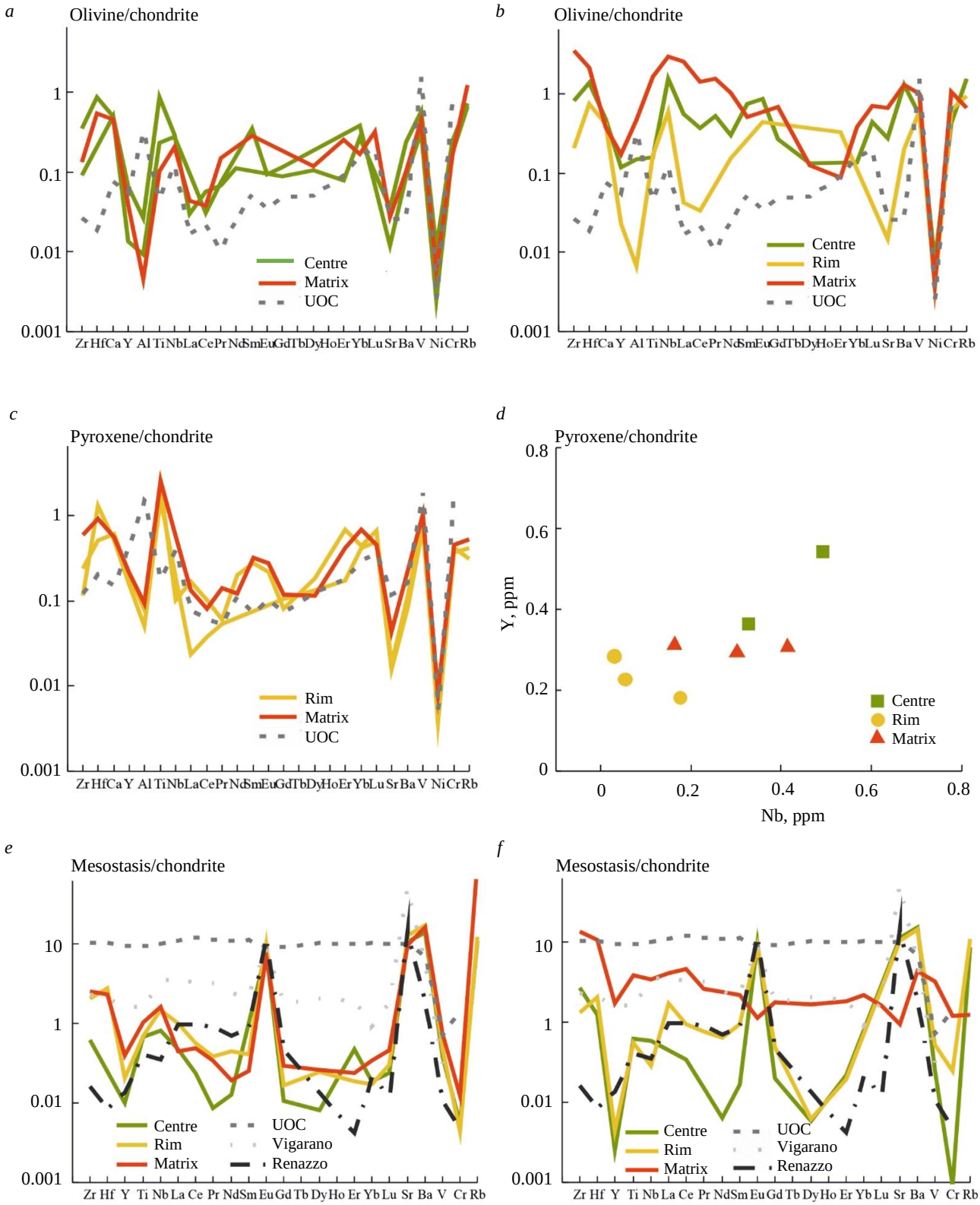


Fig.3. Spider diagrams for trace elements normalized to CI chondrite. Aggregate 14APO-3: olivine (*a*); low-Ca pyroxene (*c*) and mesostasis (*e*). Chondrule 14PO-4: olivine (*b*) and mesostasis (*f*). The Y and Nb ratio in low-Ca pyroxene of the Borodino Meteorite (*d*). Data on the composition of UOC minerals are given according to [20, 21]

This is an open access article under the CC BY 4.0 license

Low-Ca pyroxene from aggregate 14APO-3 is present as enstatite (En 81, Wo 1). It occurs as coarse fractured idiomorphic crystals overgrown with olivine grains. Its trace element concentrations are invariable, except for some minor variations: TiO_2 0.12-0.21 wt.% and Cr_2O_3 0.13-0.22 wt.%.

Trace elements in low-Ca pyroxene from aggregate 14APO-3 vary less markedly than those in olivine. Pyroxene at the aggregate rim has a minimum LREE concentration of 0.03 ppm, which is not characteristic of pyroxene from the aggregate, the matrix, and other chondrules.

Trace element distribution spectra for pyroxene from aggregate 14APO-3 are absolutely similar to each other, suggesting their permanent trace element composition (Fig.3, *c*). Trace element concentration in pyroxene from the aggregate is below chondrite values. Trace element fractionation in low-Ca pyroxene from the aggregate is not obvious.

The trace element distribution spectrum for the pyroxene of aggregate 14APO-3 has much in common with a spectrum for pyroxene from UOC. However, it contains high refractory element (Zr, Hf, Ti) and some rare-earth (Sm, Eu) element concentrations.

Mesostasis from aggregate 14APO-3 occurs very seldom. On BSE-images, it looks like absolutely homeneous plagioclase of oligoclase composition (An 11 Or 4). The major element composition of the mesostasis is stable, except for considerable variation in FeO (0.67-2.03 wt.%) and minor variations in Al_2O_3 (20.86-21.33 wt.%).

The trace element composition of mesostasis from aggregate 14APO-3 is slightly variable. The central portion of the mesostasis contains minimum trace element concentrations, especially Zr, Hf, Y and REE. Mesostasis from the aggregate rim is similar to that from the matrix, but its LREE concentrations are higher (1.50 ppm).

Trace element distribution spectra for mesostasis from the pyroxene-olivine aggregate are not differentiated (Fig.3, *e*). Trace element concentrations in the mesostasis are consistent with chondrite values. No HREE and LREE fractionation in mesostasis from the aggregate and matrix of the Borodino Meteorite has been revealed. The trace element distribution spectrum for mesostasis from the aggregate is fully consistent with that for plagioclase from Renazzo coaly chondrite. However, it contains elevated refractory Zr and Hf concentrations and low total REE.

Porphyritic chondrule 14PO-4 consists solely of olivine and mesostasis. It has a perfect rounded shape with a little nose, is small in size (500 μm) and has no silicate or metallic rims. Olivine from the chondrule occurs as coarse idiomorphic grains. The coarsest grains are up to 250 μm lengthwise, while the finest grains are 50-70 μm in size. Mesostasis is evenly distributed throughout the chondrule, it fills interstices between olivine grains and looks homogeneous on BSE-images.

Olivine from chondrule 14PO-4 is present as forsterite (Fo 81). It is coarse, highly fractured and, unlike olivine from the matrix, has well-defined facets. Major element concentrations in olivine from the chondrule are practically invariable (Table 4).

Trace elements in olivine from chondrule 14PO-4 vary markedly. For instance, olivine from the centre of the chondrule contains intermediate trace element concentrations, as compared to olivine from the rim and matrix of the meteorite. Olivine from the chondrule rim contains minimum trace element concentrations. Very low concentrations are characteristic of Y 0.03, Al 56.7, REE 0.19 and Sr 0.11 ppm. Olivine from the matrix of the Borodino Meteorite is richer in Zr, Hf and LREE than olivine from chondrule 14PO-4.

The trace element distribution spectra for olivine from chondrule 14PO-4 are poorly differentiated (Fig.3, *b*). Trace element concentrations increase to chondrite values, which are much higher than trace element concentrations in olivine from UOC. The greatest prevalence is characteristic of refractory Zr, Hf, Nb and REE. In olivine from chondrule 14PO-4, LREE dominate over HREE.

Mesostasis from chondrule 14PO-4 consists of homogeneous poorly recrystallized glass of oligoclase composition (An 11 Or 4). Plagioclase occasionally occurs together with micron-sized troilite and chromite grains. The major element composition of the mesostasis is practically invariable, except for some minor variations in FeO (0.67-2.03 wt.%).

This is an open access article under the CC BY 4.0 license

Journal of Mining Institute. 2024. Vol. 265. P. 16-33
© Kristina G. Sukhanova, 2024

Table 4

Major (wt.%) and trace (ppm) element composition of silicate minerals from 14PO-4 chondrule of the Borodino Meteorite

Component	Ol			Mes		
	Centre	Rim	Matrix	Centre	Rim	Matrix
SiO_2	39.45	39.50	39.50	64.37	64.63	–
Al_2O_3	0.00	0.00	0.00	20.86	21.33	–
MgO	42.65	43.05	42.94	0.11	0.09	–
TiO_2	0.00	0.02	0.03	0.04	0.06	–
CaO	0.03	0.04	0.02	2.44	2.47	–
FeO	17.80	17.69	17.89	2.03	0.67	–
MnO	0.47	0.47	0.48	–	–	–
Cr_2O_3	0.02	0.02	0.05	–	–	–
NiO	0.01	0.00	0.00	–	–	–
Na_2O	–	–	–	–	–	–
K_2O	–	–	–	–	–	–
Total	100.44	100.78	100.91	100.71	100.40	–
Zr	3.00	0.76	13.0	9.86	4.81	49.2
Hf	0.15	0.08	0.23	0.13	0.22	1.15
Ca	4340	3753	3513	–	–	–
Y	0.17	0.03	0.25	0.04	0.07	2.50
Al	1239	56.7	3967	–	–	–
Ti	70.4	75.4	739	281	250	1737
Nb	0.44	0.17	0.83	0.17	0.08	0.99
La	0.14	0.01	0.62	0.11	0.41	0.99
Ce	0.23	0.02	0.89	0.21	0.59	2.92
Pr	0.05	b.d.l.	0.15	0.01	0.07	0.25
Nd	0.14	0.07	0.48	0.03	0.31	1.16
Sm	0.11	b.d.l.	0.08	0.03	0.15	0.34
Eu	0.05	0.03	0.04	0.59	0.53	0.07
Gd	0.06	b.d.l.	0.14	0.04	0.10	0.37
Tb	–	–	–	–	–	–
Dy	0.03	b.d.l.	0.03	0.01	0.02	0.43
Ho	–	–	–	–	–	–
Er	b.d.l.	0.06	0.01	0.04	0.03	0.31
Yb	0.02	b.d.l.	0.06	b.d.l.	b.d.l.	0.37
Lu	0.01	b.d.l.	0.02	b.d.l.	b.d.l.	0.04
Sr	2.18	0.12	5.13	90.2	81.2	7.52
Ba	3.16	0.49	3.19	37.8	35.1	10.6
V	29.9	33.3	55.3	13.5	28.2	178
Ni	82.4	39.0	44.1	–	–	–
Cr	1111	1636	2792	24.5	648	3209
Rb	3.65	2.21	1.54	20.3	25.6	2.87
REE	0.85	0.19	2.52	1.07	2.21	7.24
LREE	0.73	0.13	2.25	0.98	2.06	5.72
HREE	0.12	0.06	0.27	0.09	0.15	1.52

Trace elements in mesostasis from chondrule 14PO-4 also vary slightly. Mesostasis contains minimum LREE concentration in the centre of the chondrule, but not at its rim. Mesostasis from the matrix has more trace and rare-earth elements than that from the chondrule, except for Eu.

The trace element distribution spectra obtained are differentiated with respect to the position of mesostasis in or outside the chondrule (Fig.3, *f*). For instance, mesostasis from the centre and at the rim of the chondrule is depleted in trace elements and displays the prevalence of LREE over HREE and a well-defined positive europium anomaly. Mesostasis from the matrix contains more trace elements than that from the chondrule, exhibits a poorly-defined negative anomaly and shows practically no light or heavy rare-earth element fractionation.

Mesostasis from the chondrule overlaps the plagioclase line for Renazzo coaly chondrite to a greater extent. However, it contains high refractory element (Zr and Hf) concentrations. Mesostasis from the matrix has a spectrum similar to that for plagioclase from Vigarano coaly chondrite. However, it contains high Zr and Hf concentrations and displays a negative europium anomaly.

This is an open access article under the CC BY 4.0 license

Discussion. Olivines from porphyritic (14POP-1 and 14PO-4) and barred 14BOP-2 chondrules, pyroxene-olivine aggregate 14APO-3 and the Borodino Meteorite matrix have practically the same trace element concentrations, but display some minor differences in trace element composition.

The trace element distribution spectrum obtained for olivine is generally poorly-differentiated. However, there is a group of olivines enriched in incompatible LREE, Sr and Ba (Fig.4, *a*, *b*). These olivines are from the different objects (chondrules and aggregate) of the meteorite, look homogeneous on BSE-images and consist of coarse (over 200 μm) grains. However, there is no difference in the trace element composition of olivine, regardless of its position in the centre of the object, at the rim or in the matrix.

Differences in the objects of the Borodino Meteorite can be seen on plots showing Ca/Ni (Fig.4, *c*) and Cr/Nb ratios (Fig.4, *d*). Olivine from barred chondrule 14BOP-2 is richer in Ca and Ni than other objects of the Borodino Meteorite, forming an isolated cloud of points. Olivine from pyroxene-olivine aggregate 14APO-3 and a barred chondrule contains more Cr and Nb than olivine from porphyritic chondrules. Olivine from the Borodino Meteorite contains more trace refractory and rare-earth elements than olivine from UOC. The bulk of olivine has less Al than UOC.

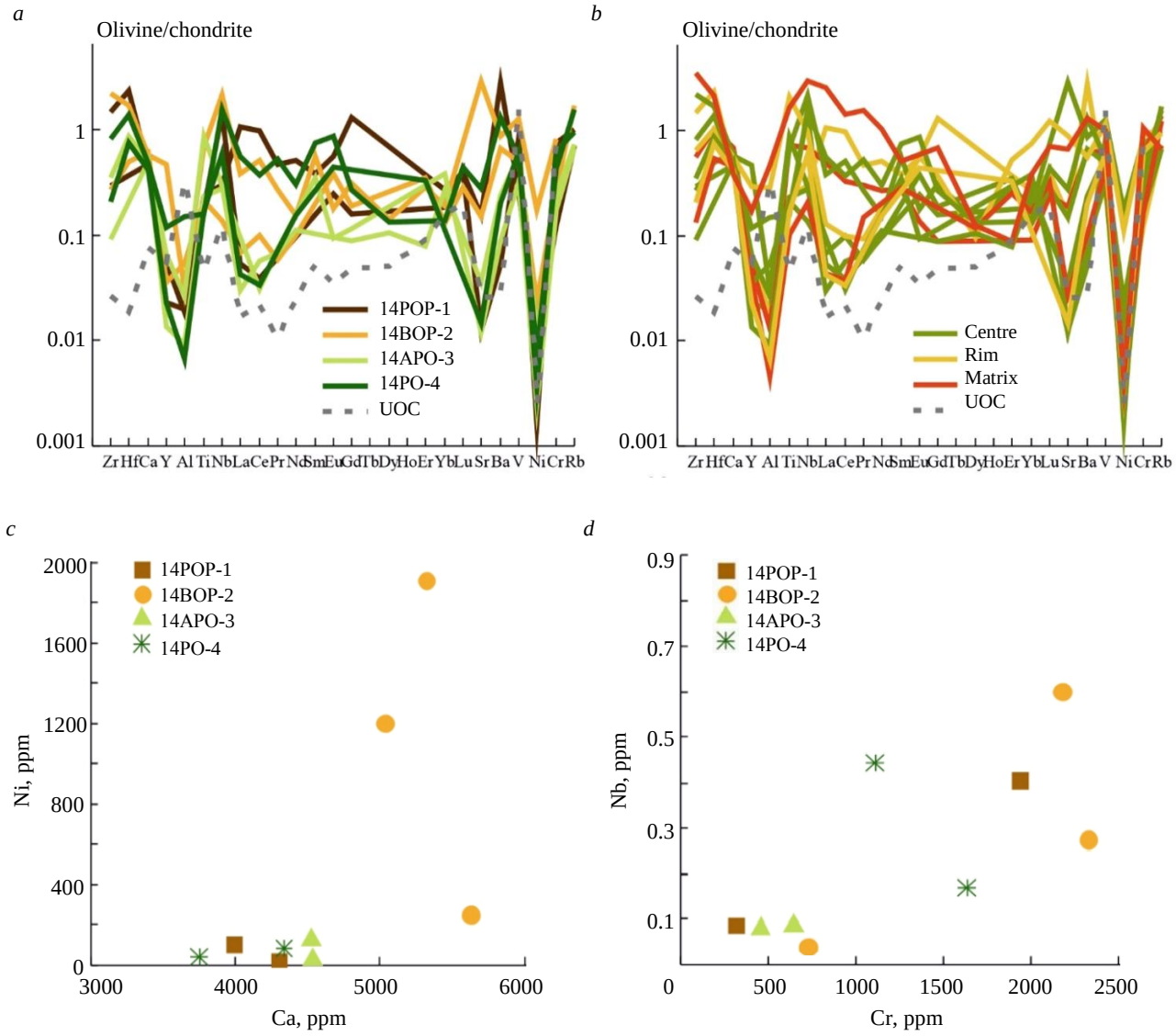


Fig.4. Spider diagrams for trace elements normalized to CI chondrite in olivine from the Borodino Meteorite relative to different chondrules (*a*) and the location of grains inside/outside the chondrule (*b*);
the Ca/Ni (*c*) and Cr /Nb (*d*) ratios. Data on the composition of UOC minerals are given according to [20, 21]

This is an open access article under the CC BY 4.0 license

Journal of Mining Institute. 2024. Vol. 265. P. 16-33
© Kristina G. Sukhanova, 2024

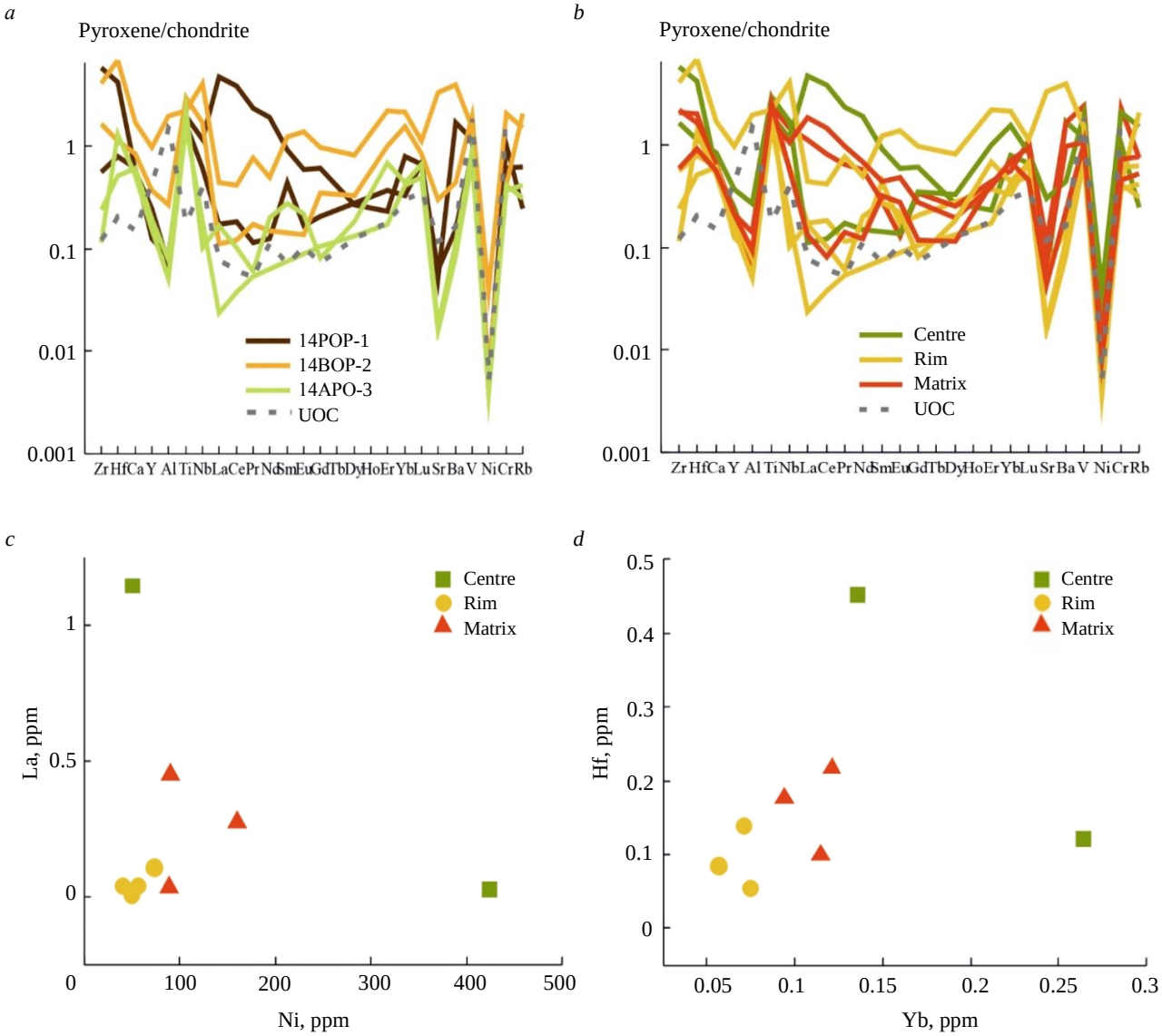


Fig.5. Spider diagrams for trace elements normalized to CI chondrite in low-Ca pyroxene from the Borodino Meteorite relative to different chondrules (*a*) and the location of grains inside/outside the chondrule (*b*);
the Ni/La (*c*) and Yb/Hf (*d*) ratios. Data on the composition of UOC minerals are given according to [20, 21]

Low-Ca pyroxene displays a variety of trace element concentrations, depending on the object in which it occurs. For instance, pyroxene from barred chondrule 14BOP-2 contains more trace elements than pyroxene from porphyritic chondrule 14POP-1 and aggregate 14APO-3 (Fig.5, *a*). Pyroxene from porphyritic chondrule 14POP-1 has low trace element concentrations. Pyroxene from the meteorite matrix is also depleted in trace elements, as compared to a barred chondrule and is more similar to pyroxene from a porphyritic chondrule (Fig.5, *b*).

Pyroxene from the Borodino Meteorite is not different from pyroxene present in porphyritic chondrules (UOC), except for a small amount of Al and high Ti concentration.

The concentration of some trace elements in low-Ca pyroxene is controlled by its position in the meteorite object. Point fields, corresponding to the position of pyroxene – in the centre, at the object rim or in the meteorite matrix, were obtained from Nb/Y (see Fig.3, *d*), Ni/La (Fig.5, *c*) and Yb/Hf (Fig.5, *d*) ratios. Thus, pyroxene from the centre of the meteorite is normally enriched in trace elements, pyroxene from the object rim is depleted in them and pyroxene from the meteorite matrix occupies an intermediate position. The trends revealed are characteristic of pyroxene from porphyritic and barred chondrules and pyroxene-olivine aggregate.

This is an open access article under the CC BY 4.0 license

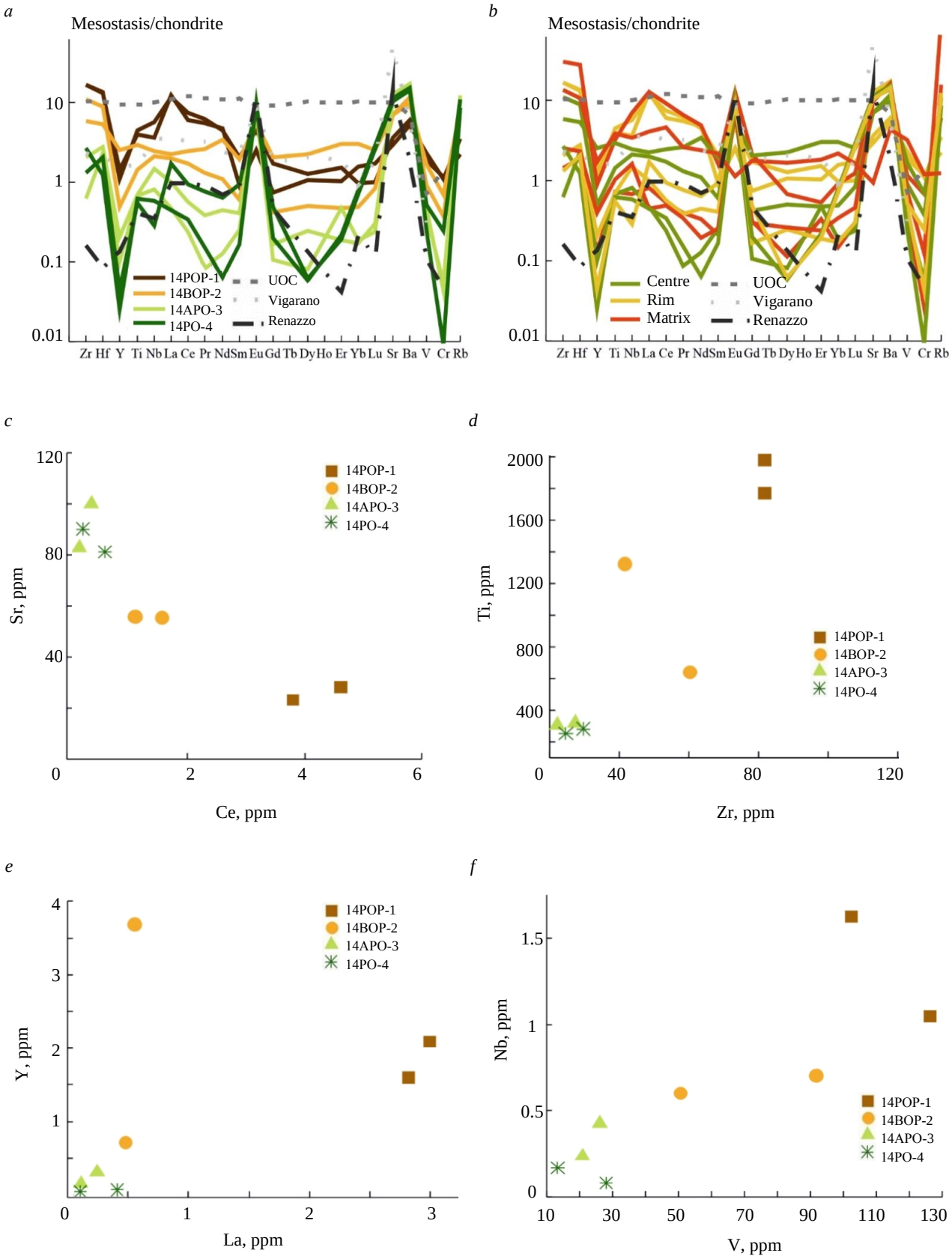


Fig.6. Spider diagrams for trace elements normalized to CI chondrite in mesostasis from the Borodino Meteorite relative to different chondrules (*a*) and the location of grains inside/outside the chondrule (*b*); the Ce/Sr (*c*), Zr/Ti (*d*), La/Y (*e*) and V/Nb (*f*) ratios. Data on the composition of UOC minerals are given according to [20, 21]

This is an open access article under the CC BY 4.0 license

Journal of Mining Institute. 2024. Vol. 265. P. 16-33
© Kristina G. Sukhanova, 2024

The trace element composition of mesostasis is more informative than the object of the meteorite in which it occurs, as compared to olivine and low-Ca pyroxene. Mesostasis from barred chondrule 14BOP-2 and porphyritic 14POP-1 chondrules is richer in trace elements than mesostasis from porphyritic chondrule 14PO-4 and pyroxene-olivine aggregate 14APO-3 (Fig.6, *a*, *b*). The trace element distribution spectrum of metostasis 14BOP-2 and 14POP-1 is either similar to that of the Vigarano Meteorite or is slightly poorer.

Mesostasis from other objects of the meteorite is depleted in trace elements and is similar to a spectrum for plagioclase from Renazzo coaly chondrite.

Differences in trace element concentrations in mesostasis between the objects of the meteorite can be seen on plots showing Ce/Sr (Fig.6, *c*), Zr/Ti (Fig.6, *d*), La/Y (Fig.6, *e*) and V/Nb (Fig.6, *f*) ratios. The first three plots show three isolated groups of points corresponding to mesostasis 14PO-4 and 14APO-3 depleted in trace elements. An intermediate position is normally occupied by mesostasis from barred chondrule 14BOP-2, and the richest mesostasis from porphyritic chondrule 14POP-1 usually occupies an opposite marginal position. The plot for Ce-Sr correlation shows an inverse ratio: mesostasis from 14PO-4 and 14APO-3 is enriched in Sr but is depleted in Ce. Mesostasis from chondrule 14POP-1 is enriched in Ce but contains minimum Sr concentration, while mesostasis from the barred chondrule occupies an intermediate position.

In spite of obvious differences in the trace element composition of mesostasis from the various objects of the Borodino Meteorite, the chemical composition of mesostasis is not controlled by its position in the object.

Conclusions. Thus, minerals from porphyritic olivine-pyroxene and barred chondrules contain elevated trace element concentrations. Trace element concentrations in olivine is correlated with grain size. The trace element composition of low-Ca pyroxene is controlled by the position of a pyroxene grain in the meteorite object, and the composition of mesostasis by the object itself. The results obtained show no traces of the equilibration of the trace element composition of silicate minerals in the Borodino Meteorite.

High LREE/HREE values for unequilibrated ordinary chondrites (UOC) are correlated with a decrease in grain size. This trend is assumed to be due to the rapid cooling of fine grains [21]. Experiments have shown that trace element accumulation in olivine and low-Ca pyroxene is intensified by an increase in chondrule crystallization rate and, hence, olivine growth rate in it. Nevertheless, the evidence obtained contradicts the earlier studies referred to in the present paper. Further studies, e.g. analysis of trace element accumulation in olivine depending on controlled by grain cross-section and estimation of the real, rather than observed, size of olivine, are needed.

Low-Ca pyroxene and mesostasis from a barred chondrule contain elevated amounts of trace elements. This evidence is consistent with experimental data indicating the rapid crystallization of chondrule melt in a protoplanetary disc. Low-Ca pyroxene shows an increase in trace element concentrations in the following sequence: rim – matrix – centre, which could be due to chondrule-nebular gas interaction [35].

The author is grateful to Candidate of Physics and Mathematics S.G.Simakin and E.V.Potapov (*Valiev IPT RAS, Yaroslavl Branch*) *for their analytical work.*

REFERENCES

1. Ivanova M.A., Nazarov M.A. History of the meteorite collection of the Russian Academy of Sciences. *Geological Society, London, Special Publications*. 2006. Vol. 256, p. 219-236. DOI: 10.1144/GSL.SP.2006.256.01.11

2. Obolonskaya E.V., Popova E.E. Meteorite Borodino. *Russkaya istoriya*. 2012. N 1, p. 95-96 (in Russian).

3. Obolonskaya E.V., Popova E.E. Meteorite collection from the Mining Museum of St. Petersburg Mining University. Meteorit Chelyabinsk – god na Zemle: Materialy Vserossiiskoi nauchnoi konferentsii, 14-15 fevralya 2014, Chelyabinsk, Rossiya. Chelyabinsk: Chelyabinskii gosudarstvennyi kraevedcheskii muzei, 2014, p. 355-363 (in Russian).

This is an open access article under the CC BY 4.0 license

4. Scott E.R.D., Krot A.N. Chondrites and Their Components. *Treatise on Geochemistry* (*Second Edition*). 2014. Vol. 1, p. 65-137. DOI: 10.1016/B978-0-08-095975-7.00104-2

5. Chondrules: Records of Protoplanetary Disk Processes. Ed. by S.S.Russell, Jr.H.C.Connolly, A.N.Krot. Cambridge: Cambridge University Press, 2018, p. 450. DOI: 10.1017/9781108284073

6. Jacquet E., Piralla M., Kersaho P., Marrocchi Y. Origin of isolated olivine grains in carbonaceous chondrites. *Meteoritics & Planetary Science*. 2021. Vol. 56. N 1, p. 13-33. DOI: 10.1111/maps.13583

7. Marrocchi Y., Euverte R., Villeneuve J. et al. Formation of CV chondrules by recycling of amoeboid olivine aggregate-like precursors. *Geochimica et Cosmochimica Acta*. 2019. Vol. 247, p. 121-141. DOI: 10.1016/j.gca.2018.12.038

8. Nardi L., Palomba E., Longobardo A. et al. Mapping olivine abundance on asteroid (25143) Itokawa from Hayabusa/NIRS data. *Icarus*. 2019. Vol. 321, p. 14-28. DOI: 10.1016/j.icarus.2018.10.035

9. Jacquet E., Marrocchi Y. Chondrule heritage and thermal histories from trace element and oxygen isotope analyses of chondrules and amoeboid olivine aggregates. *Meteoritics & Planetary Science*. 2017. Vol. 52. Iss. 12, p. 2672-2694. DOI: 10.1111/maps.12985

10. Libourel G., Krot A.N. Evidence for the presence of planetesimal material among the precursors of magnesian chondrules of nebular origin. *Earth and Planetary Science Letters*. 2007. Vol. 254. Iss. 1-2, p. 1-8. DOI: 10.1016/j.epsl.2006.11.013

11. Tenner T.J., Nakashima D., Ushikubo T. et al. Oxygen isotope ratios of FeO-poor chondrules in CR3 chondrites: Influence of dust enrichment and H_2O during chondrule formation. *Geochimica et Cosmochimica Acta*. 2015. Vol. 148, p. 228-250. DOI: 10.1016/j.gca.2014.09.025

12. Bischoff A., Schleiting M., Wieler R., Patzek M. Brecciation among 2280 ordinary chondrites – Constraints on the evolution of their parent bodies. *Geochimica et Cosmochimica Acta*. 2018. Vol. 238, p. 516-541. DOI: 10.1016/j.gca.2018.07.020

13. Grossman J.N., Brearley A.J. The onset of metamorphism in ordinary and carbonaceous chondrites. *Meteoritics & Planetary Science*. 2005. Vol. 40. Iss. 1, p. 87-122. DOI: 10.1111/j.1945-5100.2005.tb00366.x

14. Chakraborty S. Diffusion Coefficients in Olivine, Wadsleyite and Ringwoodite. *Reviews in Mineralogy and Geochemistry*. 2010. Vol. 72. N 1, p. 603-639. DOI: 10.2138/rmg.2010.72.13

15. Cherniak D.J. REE diffusion in olivine. *American Mineralogist*. 2010. Vol. 95. N 2-3, p. 362-368. DOI: 10.2138/am.2010.3345

16. Pape J., Mezger K., Bouvier A.-S., Baumgartner L.P. Time and duration of chondrule formation: Constraints from ^{26}Al-^{26}Mg ages of individual chondrules. *Geochimica et Cosmochimica Acta*. 2019. Vol. 244, p. 416-436. DOI: 10.1016/j.gca.2018.10.017

17. Marrocchi Y., Villeneuve J., Batanova V. et al. Oxygen isotopic diversity of chondrule precursors and the nebular origin of chondrules. *Earth and Planetary Science Letters*. 2018. Vol. 496, p. 132-141. DOI: 10.1016/j.epsl.2018.05.042

18. Piralla M., Villeneuve J., Batanova V. et al. Conditions of chondrule formation in ordinary chondrites. *Geochimica et Cosmochimica Acta*. 2021. Vol. 313, p. 295-312. DOI: 10.1016/j.gca.2021.08.007

19. Varela M.E. Bulk trace elements of Mg-rich cryptocrystalline and ferrous radiating pyroxene chondrules from Acfer 182: Their evolution paths. *Geochimica et Cosmochimica Acta*. 2019. Vol. 257, p. 1-15. DOI: 10.1016/j.gca.2019.04.025

20. Jacquet E., Alard O., Gounelle M. Trace element geochemistry of ordinary chondrite chondrules: The type I/type II chondrule dichotomy. *Geochimica et Cosmochimica Acta*. 2015. Vol. 155, p. 47-67. DOI: 10.1016/j.gca.2015.02.005

21. Jacquet E., Alard O., Gounelle M. Chondrule trace element geochemistry at the mineral scale. *Meteoritics & Planetary Science*. 2012. Vol. 47. N 11, p. 1695-1714. DOI: 10.1111/maps.12005

22. Jacquet E., Alard O., Gounelle M. The formation conditions of enstatite chondrites: Insights from trace element geochemistry of olivine-bearing chondrules in Sahara 97096 (EH3). *Meteoritics & Planetary Science*. 2015. Vol. 50. N 9, p. 1624-1642. DOI: 10.1111/maps.12481

23. Varela M.E., Sylvester P., Brandstätter F., Engler A. Nonporphyritic chondrules and chondrule fragments in enstatite chondrites: Insights into their origin and secondary processing. *Meteoritics & Planetary Science*. 2015. Vol. 50. N 8, p. 1338-1361. DOI: 10.1111/maps.12468

24. Skublov S.G., Rumyantseva N.A., Vanshtein B.G. et al. Zircon Xenocrysts from the Shaka Ridge Record Ancient Continental Crust: New U-Pb Geochronological and Oxygen Isotopic Data. *Journal of Earth Science*. 2022. Vol. 33. N 1, p. 5-16. DOI: 10.1007/s12583-021-1422-2

25. Rumyantseva N.A., Skublov S.G., Vanshteina B.G. et al. Zircon from Gabbroids of the Shaka Ridge (South Atlantic): U-Pb Age, Oxygen Isotope Ratios and Trace Element Composition. *Proceedings of the Russian Mineralogical Society*. 2022. Part CLI. N 1, p. 44-73 (in Russian). DOI: 10.31857/S0869605522010099

26. Skublov S.G., Gavrilchik A.K., Berezin A.V. Geochemistry of beryl varieties: comparative analysis and visualization of analytical data by principal component analysis (PCA) and t-distributed stochastic neighbor embedding (t-SNE). *Journal of Mining Institute*. 2022. Vol. 255, p. 455-469. DOI: 10.31897/PMI.2022.40

27. Gavrilchik A.K., Skublov S.G., Kotova E.L. Trace Element Composition of Beryl From the Sherlovaya Gora Deposit, South-Eastern Transbaikalia, Russia. *Proceedings of the Russian Mineralogical Society*. 2021. Part CL. N 2, p. 69-82 (in Russian). DOI: 10.31857/S0869605521020052

28. Ashikhmin D.S., Skublov S.G., Melnik A.E. et al. Geochemistry of Rock-Forming Minerals in Mantle Xenoliths from Basalts of Sverre Volcano, Spitsbergen Archipelago. *Geochemistry International*. 2018. Vol. 56, p. 857-864. DOI: 10.1134/S0016702918080025

29. Sukhanova K.G., Kuznetsov A.B., Galankina O.L. Features of olivine crystallization in ordinary chondrites (Saratov meteorite): geochemistry of trace and rare earth elements. *Journal of Mining Institute*. 2022. Vol. 254, p. 149-157. DOI: 10.31897/PMI.2022.39

30. Sukhanova K.G., Skublov S.G., Galankina O.L. et al. Trace Element Composition of Silicate Minerals in the Chondrules and Matrix of the Buschhof Meteorite. *Geochemistry International*. 2020. Vol. 58, p. 1321-1330. DOI: 10.1134/S001670292012006X

This is an open access article under the CC BY 4.0 license

Journal of Mining Institute. 2024. Vol. 265. P. 16-33
© Kristina G. Sukhanova, 2024

31. Sukhanova K.G. Silicate minerals composition as a reflection of equilibrated ordinary chondrite evolution: Avtoref. dis. … kand. geol.-mineral. nauk. Moscow: Moskovskii gosudarstvennyi universitet, 2022, p. 21 (in Russian).

32. Zanetta P.-M., Le Guillou C., Leroux H. et al. Modal abundance, density and chemistry of micrometer-sized assemblages by advanced electron microscopy: Application to chondrites. *Chemical Geology*. 2019. Vol. 514, p. 27-41. DOI: 10.1016/j.chemgeo.2019.03.025

33. Portnyagin M., Almeev R., Matveev S., Holtz F. Experimental evidence for rapid water exchange between melt inclusions in olivine and host magma. *Earth and Planetary Science Letters*. 2008. Vol. 272. Iss. 3-4, p. 541-552. DOI: 10.1016/j.epsl.2008.05.020

34. Palme H., Lodders K., Jones A. Solar System Abundances of the Elements. *Treatise on Geochemistry* (*Second Edition*). 2014. Vol. 2, p. 15-36. DOI: 10.1016/b978-0-08-095975-7.00118-2

35. Engler A., Varela M.E., Kurat G. et al. The origin of non-porphyritic pyroxene chondrules in UOCs: Liquid solar nebula condensates? *Icarus*. 2007. Vol. 192. Iss. 1, p. 248-286. DOI: 10.1016/j.icarus.2007.06.016

***Author* Kristina G. Sukhanova,** *Candidate of Geological and Mineralogical Sciences, Junior Researcher, cris.suhanova92@yandex.ru, https://orcid.org/0000-0001-5695-0767* (*Institute of Precambrian Geology and Geochronology RAS, Saint Petersburg, Russia*).

The author declares no conflict of interests.

This is an open access article under the CC BY 4.0 license